

# Efficient Image Super-Resolution with Multi-Scale Spatial Adaptive Attention Networks

Sushi Rao

Zhejiang Gongshang University  
25090672@mail.zjgsu.edu

Jingwei Li

Zhejiang Gongshang University  
25090246@mail.zjgsu.edu

## Abstract

This paper introduces a lightweight image super-resolution (SR) network, termed the Multi-scale Spatial Adaptive Attention Network (MSAAN), to address the common dilemma between high reconstruction fidelity and low model complexity in existing SR methods. The core of our approach is a novel Multi-scale Spatial Adaptive Attention Module (MSAA), designed to jointly model fine-grained local details and long-range contextual dependencies. The MSAA comprises two synergistic components: a Global Feature Modulation Module (GFM) that learns coherent texture structures through differential feature extraction, and a Multi-scale Feature Aggregation Module (MFA) that adaptively fuses features from local to global scales using pyramidal processing. To further enhance the network’s capability, we propose a Local Enhancement Block (LEB) to strengthen local geometric perception and a Feature Interactive Gated Feed-Forward Module (FIGFF) to improve nonlinear representation while reducing channel redundancy. Extensive experiments on standard benchmarks (Set5, Set14, B100, Urban100, Manga109) across  $\times 2$ ,  $\times 3$ , and  $\times 4$  scaling factors demonstrate that both our lightweight (MSAAN-light) and standard (MSAAN) versions achieve superior or competitive performance in terms of PSNR and SSIM, while maintaining significantly lower parameters and computational costs than state-of-the-art methods. Ablation studies validate the contribution of each component, and visual results show that MSAAN reconstructs sharper edges and more realistic textures.

## 1 Introduction

Image Super-Resolution (SR) is a pivotal task in computer vision, aiming to reconstruct a High-Resolution (HR) image from its degraded Low-Resolution (LR) counterpart [1, 2]. This technology is crucial for numerous practical applications, including medical imaging, surveillance, and remote sensing, where

acquisition hardware or sensor limitations often result in images lacking fine details.

The advent of deep learning has significantly propelled the field forward, with Convolutional Neural Network (CNN)-based models achieving remarkable reconstruction performance [3, 4, 5]. However, a common strategy to enhance performance involves stacking numerous convolutional layers, which inevitably leads to high computational complexity and a large number of parameters. In response, researchers have developed various lightweight CNN-based SR methods, such as CARN [6], IMDN [7], RFDN [8], LAPAR [5], and ShuffleMixer [9]. Despite their efficiency, these methods are fundamentally limited by the local receptive field of convolution operations, which hinders their ability to model long-range dependencies—a key factor in recovering intricate textures and structures.

Recently, Vision Transformers (ViT) [10] have demonstrated superior capability in capturing long-range, non-local interactions through self-attention mechanisms, leading to promising results in low-level vision tasks like image restoration [11, 12]. This has inspired a new direction towards Transformer-based lightweight SR methods, including ESRT [13], LBNNet [14], and SAFMN [15]. Nevertheless, effectively and efficiently integrating the local high-frequency detail perception of CNNs with the global contextual modeling of Transformers remains a significant challenge. Many existing approaches still exhibit limitations in harmonizing these two complementary capabilities, often resulting in suboptimal reconstruction of fine details or excessive model complexity.

Inspired by the inherent self-similarity within natural images—where reconstructing one region can benefit from referencing similar patches elsewhere—it is imperative for an SR model to capture both short-range local details and long-range dependencies [16, 17, 18, 19]. The core challenge, therefore, lies in designing an efficient architecture that seamlessly unifies these dual modeling capacities under strict computational constraints.

To address this challenge, we propose a novel Multi-scale Spatial Adaptive Attention Network (MSAAN) for lightweight image super-resolution. The cornerstone of our network is a custom-designed Multi-scale Spatial Adaptive Attention Module (MSAA). This module is engineered to explicitly and efficiently model features across different scales and spatial locations. The MSAA integrates a Global Feature Modulation module (GFM) that learns coherent texture structures and a Multi-scale Feature Aggregation module (MFA) that adaptively fuses features from local to global contexts. To further refine the network, we introduce a Local Enhancement Block (LEB) to bolster the modeling of local geometric patterns and a Feature Interactive Gated Feed-Forward module (FIGFF) to enhance nonlinear representational capacity while reducing channel redundancy. Comprehensive experiments demonstrate that MSAAN achieves an excellent balance between reconstruction quality and model efficiency, outperforming state-of-the-art methods on standard benchmarks.

The main contributions of this work are summarized as follows:

- We propose a novel Multi-scale Spatial Adaptive Attention Network (MSAAN),

a lightweight yet powerful architecture for image super-resolution.

- We design a core Multi-scale Spatial Adaptive Attention Module (MSAA) that effectively unifies global texture modulation and adaptive multi-scale feature aggregation.
- We introduce auxiliary components, including a Local Enhancement Block (LEB) and a Feature Interactive Gated Feed-Forward module (FIGFF), to strengthen local detail capture and improve feature transformation efficiency.
- Extensive experiments validate that both our lightweight (MSAAN-light) and standard (MSAAN) models set new state-of-the-art performance across multiple datasets and scale factors while maintaining low complexity.

## 2 Related Works

### 2.1 CNN-based Lightweight Super-Resolution

With the advancement of deep learning, Convolutional Neural Network (CNN)-based methods have become dominant in the field of image super-resolution (SR) due to their powerful feature extraction capabilities [20, 21]. Early deep SR models often stacked a large number of layers to enhance performance, which significantly increased computational cost and model parameters. To address this efficiency challenge, a series of lightweight CNN architectures have been proposed. Ahn et al. [6] introduced the Cascading Residual Network (CARN), which combines group convolution and a cascading structure of residual blocks to effectively capture complex image details. Hui et al. proposed the Information Distillation Network (IDN) [22] and its enhanced version, the Information Multi-distillation Network (IMDN) [23], which employ information distillation blocks to extract hierarchical features, achieving a good balance between parameter compression and performance. Building upon IMDN, Liu et al. [24] proposed the Residual Feature Distillation Network (RFDN), which introduces Feature Distillation Connections (FDC) to further reduce network complexity. Li et al. [25, 3, 26, 27] designed the Linearly-Assembled Pixel-Adaptive Regression Network (LAPAR), transforming the mapping from LR to HR images into a linear coefficient regression task based on predefined filter bases. Kong et al. [28] simplified the feature aggregation process in RFDN and proposed the Residual Local Feature Network (RLFN) for faster inference. Sun et al. [29] introduced the Shuffle-Mixer, which utilizes large convolutional kernels to aggregate spatial information with an enlarged receptive field while reducing parameters and FLOPs. Although these CNN-based lightweight methods achieve impressive performance, their inherent locality limits their ability to model long-range dependencies, potentially restricting detail recovery.

## 2.2 Transformer-based Super-Resolution

The Vision Transformer (ViT) [30] has demonstrated remarkable success in various computer vision tasks, including low-level vision, due to its superior capability in capturing non-local feature interactions [31, 32]. This has motivated researchers to explore Transformer architectures for image SR. Lu et al. [33] proposed the Efficient Super-Resolution Transformer (ESRT), which reduces computational cost while preserving high-frequency information. Gao et al. [34, 35] introduced the Lightweight Bimodal Network (LBNet), which employs a recursive mechanism to deepen the Transformer without adding parameters, thereby capturing long-range dependencies to facilitate detail and texture reconstruction. Sun et al. [9] designed the Spatially-Adaptive Feature Modulation Network (SAFMN), which incorporates a Spatially-Adaptive Feature Modulation (SAFM) block to dynamically select representative features, achieving Transformer-like effects at a lower computational cost.

## 2.3 Motivation and Contribution

Existing methods, including ESRT [36], LBNet [37], and SAFMN [38], have made significant progress in lightweight SR. However, as noted in the document, their ability to jointly model high-frequency local details and long-range dependencies remains limited, which can lead to suboptimal reconstruction quality. Effectively integrating these two complementary capabilities under constrained computational resources is crucial for precise image restoration.

Inspired by the self-similarity within images—where reconstructing one region can benefit from referencing similar patches elsewhere—it is essential to capture both short-range and long-range pixel relationships [39, 8, 40]. To this end, we propose the Multi-scale Spatial Adaptive Attention Network (MSAAN). Our work distinguishes itself by designing a dedicated Multi-scale Spatial Adaptive Attention Module (MSAA) that explicitly and efficiently unifies global texture modulation and adaptive multi-scale local feature aggregation. Furthermore, we introduce auxiliary components like the Local Enhancement Block (LEB) and the Feature Interactive Gated Feed-Forward Module (FIGFF) to strengthen local detail perception and improve feature transformation efficiency. As demonstrated by subsequent experiments, MSAAN achieves a superior balance between reconstruction performance and model complexity.

# 3 Methodology

## 3.1 Overall Architecture

The proposed Multi-scale Spatial Adaptive Attention Network (MSAAN) is designed to achieve high-quality image super-resolution while maintaining a lightweight structure. The overall framework, as depicted in Figure 1, comprises three primary components: the Shallow Feature Extraction Module (SFEM),

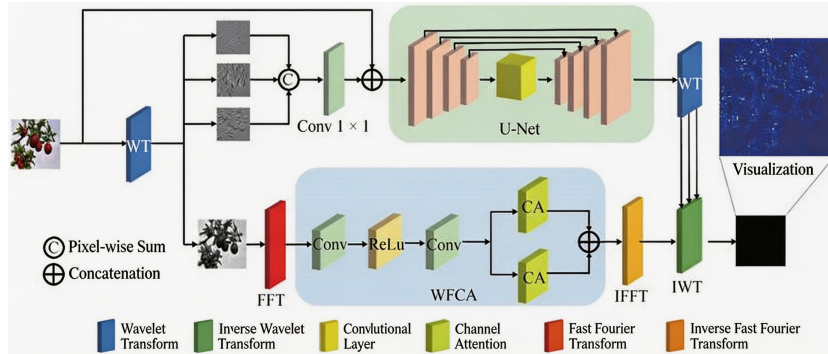


Figure 1: Overall architecture of MSAAN

the Deep Feature Extraction Module (DFEM), and the Image Reconstruction Module (IRM).

Given a low-resolution input image  $I_{LR} \in \mathbb{R}^{3 \times H \times W}$ , the network first employs the SFEM, which consists of a single  $3 \times 3$  convolutional layer, to extract initial shallow features:

$$F_0 = H_{\text{SFEM}}(I_{LR}) \in \mathbb{R}^{C \times H \times W}, \quad (1)$$

where  $H_{\text{SFEM}}(\cdot)$  denotes the operation of the SFEM.

These shallow features are then fed into the DFEM, the core of MSAAN responsible for extracting rich hierarchical representations. The DFEM is constructed by stacking  $n$  Spatial Feature Mixers (SFMs):

$$F_i = H_{\text{SFM}_i}(F_{i-1}), \quad i = 1, 2, \dots, n, \quad (2)$$

where  $H_{\text{SFM}_i}(\cdot)$  represents the function of the  $i$ -th SFM. A global residual connection is incorporated to facilitate the learning of high-frequency details and ease gradient flow, yielding the final deep feature:

$$F_{DF} = F_n + F_0. \quad (3)$$

Finally, the IRM reconstructs the high-resolution output image from  $F_{DF}$ . The IRM is implemented as a lightweight upsampling layer, containing a  $3 \times 3$  convolution followed by a PixelShuffle operation [41]. A skip connection from the bilinearly upsampled input image is added to aid convergence and enhance performance:

$$I_{SR} = H_{\text{Upsample}}(F_{DF}) + \text{bilinear}(I_{LR}), \quad (4)$$

where  $H_{\text{Upsample}}(\cdot)$  is the upsampling module and  $\text{bilinear}(\cdot)$  denotes bilinear interpolation.

### 3.2 Spatial Feature Mixer (SFM)

The Spatial Feature Mixer (SFM) serves as the fundamental building block of the DFEM, designed to effectively integrate local details with global context.

As shown in Figure 1, each SFM sequentially processes input features through three key sub-modules: a Local Enhancement Block (LEB), a Multi-scale Spatial Adaptive Attention Module (MSAA), and a Feature Interactive Gated Feed-Forward Module (FIGFF). For an input feature map  $X \in \mathbb{R}^{C \times H \times W}$ , the output  $Y_{\text{SFM}}$  is computed as follows:

$$Z_1 = H_{\text{LEB}}(X), \quad (5)$$

$$Z_2 = H_{\text{MSAA}}(\text{LN}(Z_1)) + Z_1, \quad (6)$$

$$Y_{\text{SFM}} = H_{\text{FIGFF}}(\text{LN}(Z_2)) + Z_2, \quad (7)$$

where  $\text{LN}(\cdot)$  denotes Layer Normalization [42].  $H_{\text{LEB}}(\cdot)$ ,  $H_{\text{MSAA}}(\cdot)$ , and  $H_{\text{FIGFF}}(\cdot)$  represent the functions of the LEB, MSAA, and FIGFF modules, respectively.

### 3.2.1 Local Enhancement Block (LEB)

To strengthen the network’s ability to model local geometric patterns without significant computational overhead, we propose a lightweight Local Enhancement Block (LEB). Inspired by the role of relative position embeddings in enhancing local modeling within vision transformers [41], the LEB acts as an efficient form of positional encoding. It is implemented as a  $3 \times 3$  depthwise convolution with a residual connection:

$$Y_{\text{LEB}} = H_{\text{DWConv}_{3 \times 3}}(X) + X, \quad (8)$$

where  $H_{\text{DWConv}_{3 \times 3}}(\cdot)$  denotes the depthwise convolution operation. This design augments local feature representation with minimal parameter addition.

### 3.2.2 Multi-scale Spatial Adaptive Attention Module (MSAA)

The Multi-scale Spatial Adaptive Attention Module (MSAA) is the core innovation for capturing and fusing features across multiple spatial scales. It consists of two cascaded components: the Global Feature Modulation Module (GFM) and the Multi-scale Feature Aggregation Module (MFA).

$$Y_{\text{MSAA}} = H_{\text{MFA}}(H_{\text{GFM}}(X)). \quad (9)$$

**Global Feature Modulation Module (GFM):** The GFM aims to modulate input features to enhance the continuity and diversity of global texture representations. It employs a differential feature extraction strategy [43]. First, initial features  $X_1 = H_{\text{Conv}_{1 \times 1}}(X)$  are extracted via a  $1 \times 1$  convolution. A global context vector is obtained through Global Average Pooling (GAP). The difference between the local features  $X_1$  and this global context is computed, scaled by a learnable parameter  $\gamma$  (initialized to 0), and used for feature reweighting. The result is fused with the original features and activated by a GeLU function [44]:

$$M_1 = H_{\text{GeLU}}(X_1 + \gamma \odot (X_1 - \text{GAP}(X_1))). \quad (10)$$

This process dynamically suppresses less informative interactions, allowing the network to focus on learning balanced global representations.

**Multi-scale Feature Aggregation Module (MFA):** The MFA is designed to adaptively aggregate features from local to global scales. To maintain efficiency, the input feature  $M_1$  is first split into four groups along the channel dimension:  $[X_0, X_1, X_2, X_3] = H_{\text{Split}}(M_1)$ .

Each group undergoes a scale-specific processing path. For the  $i$ -th group, an adaptive max pooling operation with stride  $2^i$  downsamples the feature to simulate a larger receptive field. A  $3 \times 3$  depthwise convolution extracts features at this scale, which are then upsampled back to the original resolution  $s$  via nearest-neighbor interpolation:

$$\widehat{X}_i = H_{\uparrow s} \left( H_{\text{DWConv}_{3 \times 3}} \left( H_{\downarrow \frac{s}{2^i}}(X_i) \right) \right), \quad i = 0, 1, 2, 3. \quad (11)$$

The processed features from all four scales are concatenated, combining fine-grained local details with coarse-grained semantic information. A  $1 \times 1$  convolution fuses them:

$$\widehat{X} = H_{\text{Conv}_{1 \times 1}} \left( H_{\text{Concat}}([\widehat{X}_0, \widehat{X}_1, \widehat{X}_2, \widehat{X}_3]) \right). \quad (12)$$

Subsequently, a spatially adaptive attention map is generated. Both the aggregated multi-scale feature  $\widehat{X}$  and a separately processed version of  $M_1$  (via a  $1 \times 1$  conv and GeLU) are transformed by GeLU activation. Their element-wise multiplication produces a channel-attentive map that highlights important features. A final  $1 \times 1$  convolution yields the output:

$$Y = H_{\text{Conv}_{1 \times 1}} \left( H_{\text{GeLU}}(\widehat{X}) \odot H_{\text{GeLU}}(H_{\text{Conv}_{1 \times 1}}(M_1)) \right), \quad (13)$$

where  $\odot$  denotes element-wise multiplication. This enables the MSAA to holistically integrate multi-scale context, local details, and long-range dependencies.

### 3.2.3 Feature Interactive Gated Feed-Forward Module (FIGFF)

We redesign the standard transformer feed-forward network to be more efficient for image SR. The proposed Feature Interactive Gated Feed-Forward Module (FIGFF) incorporates shift convolution (Shift-Conv) [28] and a feature gating (FG) mechanism.

The input  $X$  first passes through a Shift-Conv layer and a GeLU activation:  $Z = H_{\text{GeLU}}(H_{\text{Shift-Conv}}(X))$ . The feature  $Z$  is then split into two channel groups:  $[\widehat{Z}_1, \widehat{Z}_2] = H_{\text{Split}}(Z)$ . One branch ( $\widehat{Z}_2$ ) is refined by a  $3 \times 3$  depthwise convolution. The other branch ( $\widehat{Z}_1$ ) interacts with the refined features via element-wise multiplication, promoting cross-feature information exchange:

$$\widehat{Z} = \widehat{Z}_1 \odot H_{\text{DWConv}_{3 \times 3}}(\widehat{Z}_2). \quad (14)$$

A final Shift-Conv layer produces the output:

$$Y_{\text{FIGFF}} = H_{\text{Shift-Conv}}(\hat{Z}). \quad (15)$$

The FG mechanism reduces channel redundancy and selectively enhances critical features, improving local feature extraction with low computational cost.

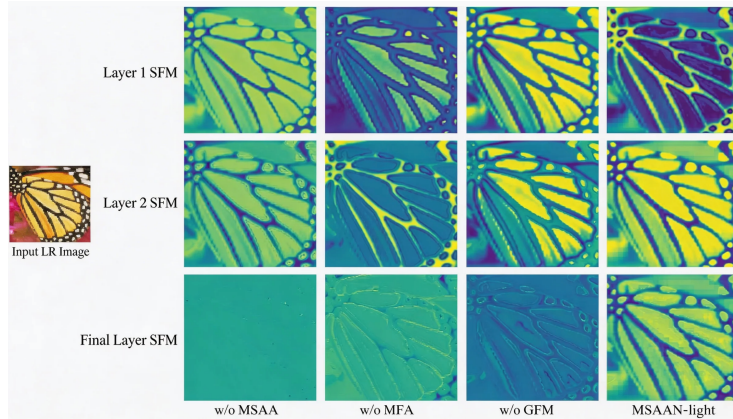


Figure 2: Visualization of feature maps before and after MSAA removal

## 4 Experiments and Results

### 4.1 Experimental Settings

**Datasets and Metrics.** The models are trained on the Flickr2K [45] and DIV2K [46] datasets, containing 800 and 2650 training images, respectively. Low-Resolution (LR) images are generated by applying bicubic downsampling to the High-Resolution (HR) references. For evaluation, we employ five standard benchmark datasets: Set5 [47], Set14 [48], B100 [49], Urban100 [7], and Manga109 [50]. The reconstruction quality is assessed using Peak Signal-to-Noise Ratio (PSNR) and Structural Similarity Index (SSIM) calculated on the luminance (Y) channel after converting images to YCbCr color space. Model complexity is measured by the number of parameters and Floating-Point Operations (FLOPs).

**Model Configurations and Training Details.** We train two versions of our network: a lightweight version *MSAAN-light* (12 SFMs, 40 channels) and a standard version *MSAAN* (24 SFMs, 60 channels). During training, random patches of size  $64 \times 64$  and  $48 \times 48$  are cropped from LR images for *MSAAN-light* and *MSAAN*, respectively. Standard data augmentation techniques, including random horizontal flipping and rotation, are applied. Both models are optimized using the Adam optimizer [4] ( $\beta_1 = 0.9$ ,  $\beta_2 = 0.99$ ). The initial learning

rate is set to  $1 \times 10^{-3}$  for MSAAN-light and  $3 \times 10^{-4}$  for MSAAN, and is decayed following a cosine annealing schedule [29]. The loss function is a weighted combination of L1 loss and a Fast Fourier Transform (FFT)-based frequency loss [51]:  $\mathcal{L} = \mathcal{L}_1 + 0.05 \cdot \mathcal{L}_{FFT}$ . All experiments are conducted using PyTorch on NVIDIA RTX 3090 GPUs.

## 4.2 Ablation Studies

Ablation studies are performed on the Set5 and Urban100 datasets with a scale factor of  $\times 4$ , using the MSAAN-light configuration to validate the effectiveness of each proposed component.

**Number of SFMs.** We investigate the impact of the number of stacked Spatial Feature Mixers (SFMs). As shown in Table 1, performance improves as the number of SFMs increases from 8 to 12. Beyond 12 SFMs, the performance gain becomes marginal or even slightly decreases, indicating that 12 SFMs represent a good balance between network depth and feature representation capacity for our lightweight design.

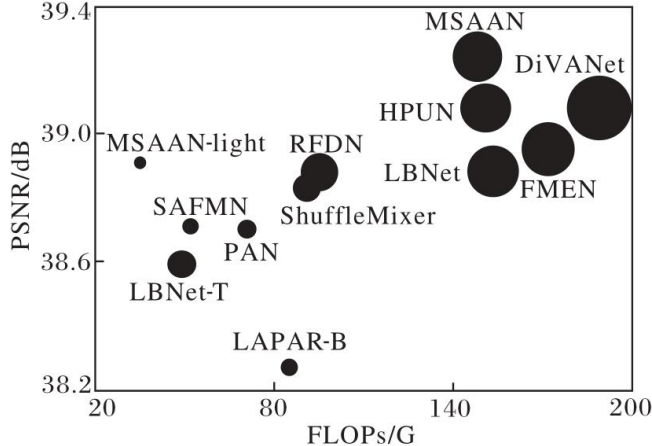


Figure 3: Comparison of metric values for different methods on the Manga109 dataset at a scale factor of  $\times 2$

**Effectiveness of LEB.** The contribution of the Local Enhancement Block (LEB) is analyzed in Table 2. Adding the LEB improves PSNR by 0.04 dB and 0.06 dB on Set5 and Urban100, respectively, for MSAAN-light, with a negligible parameter increase of only 0.5K. A similar positive effect is observed when integrating LEB into SAFMN [52], confirming its general utility in enhancing local geometric modeling.

**Effectiveness of MSAA Components.** We ablate the two core components of the Multi-scale Spatial Adaptive Attention Module (MSAA): the Global Feature Modulation Module (GFM) and the Multi-scale Feature Aggregation Module (MFA). Results in Table 3 demonstrate that removing either GFM or

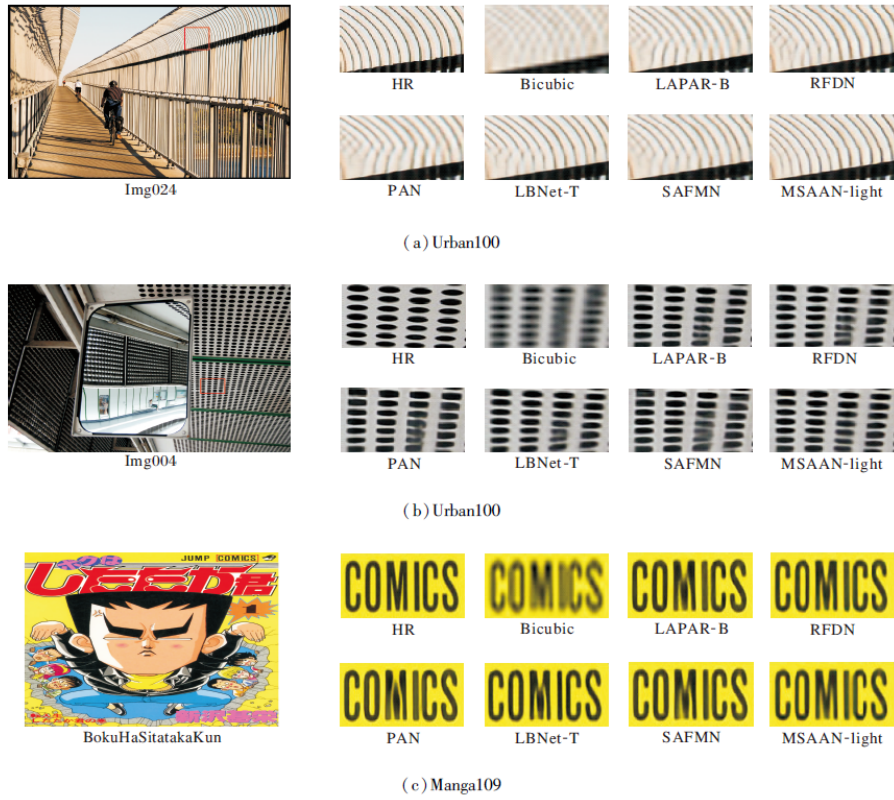


Figure 4: Visualization results of MSAAN-light and contrastive methods at a magnification factor of 4

MFA leads to performance degradation. The complete MSAAN module achieves the best results, verifying that GFM and MFA work synergistically; GFM provides well-modulated global context, while MFA enables effective multi-scale feature fusion.

**Effectiveness of FIGFF and FG Mechanism.** Table 4 shows that replacing a standard MLP with our Feature Interactive Gated Feed-Forward Module (FIGFF) yields better performance. Furthermore, ablating the Feature Gating (FG) mechanism within FIGFF, as shown in Table 5, not only increases parameters and FLOPs but also degrades performance. This validates that the FG mechanism is crucial for reducing channel redundancy and facilitating beneficial feature interactions.

### 4.3 Comparative Experiments

#### 4.3.1 Quantitative Comparisons

We compare MSAAN-light with several state-of-the-art lightweight SR methods: RFDN [53], LAPAR-B [54], PAN [55], ShuffleMixer [56], LBNNet-T [57], and SAFMN [58]. The standard MSAAN is compared against larger models: LatticeNet [55], HPUN [30], DiVANet [59], ESRT [33], LBNNet [60], FMEN [3], and NGswin [61].

The PSNR/SSIM results for scale factors  $\times 2$ ,  $\times 3$ , and  $\times 4$  are comprehensively listed in Tables 6 to 11. The key findings are summarized as follows:

- **MSAAN-light vs. Lightweight Methods:** MSAAN-light consistently outperforms all competing lightweight methods across all scales and datasets while possessing fewer parameters and FLOPs. For instance, on the Manga109 dataset at  $\times 3$  scaling (Table 7), MSAAN-light surpasses RFDN, PAN, and ShuffleMixer by 0.13 dB, 0.19 dB, and 0.11 dB in PSNR, respectively, with 68%, 33%, and 58% fewer parameters.
- **MSAAN vs. Larger Models:** As shown in Tables 9, 10, and 11, MSAAN achieves superior or highly competitive performance compared to models with comparable or even greater complexity. For example, on Manga109 at  $\times 3$  (Table 10), MSAAN outperforms ESRT, DiVANet, and NGswin by 0.28 dB, 0.29 dB, and 0.34 dB, respectively.

These results demonstrate that MSAAN achieves an excellent trade-off between reconstruction quality and model efficiency.

#### 4.3.2 Visual Comparisons

Visual results for  $\times 4$  SR are presented in Figure 4 (comparing MSAAN-light with other lightweight methods) and Figure 5 (comparing MSAAN with larger models). The proposed methods reconstruct images with sharper edges and more accurate textures. For example, in images containing regular patterns (e.g., stripes in ‘img\_024’) or dense structures (e.g., ‘img\_004’ and ‘img\_011’),

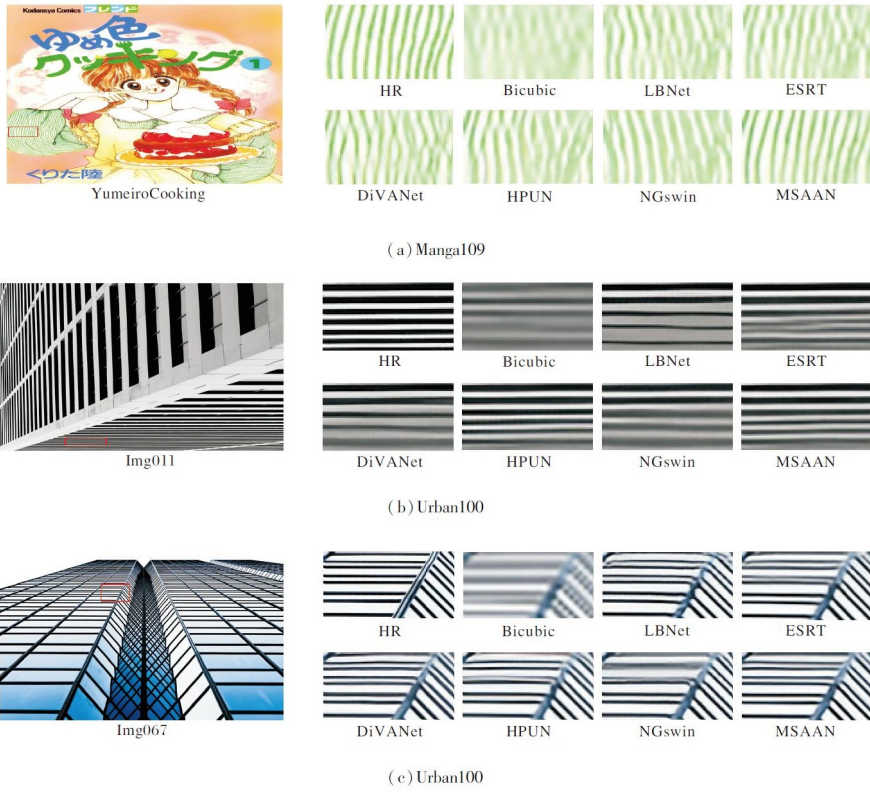


Figure 5: Visualization results of MSAAN and contrastive methods at a magnification factor of 4

MSAAN and MSAAN-light recover clearer and more consistent details compared to other methods, where results often appear blurry or contain artifacts.

### 4.3.3 Analysis via Local Attribution Maps

To understand which pixels contribute most to the reconstruction, we visualize Local Attribution Maps (LAM) [62] and compute the Diffusion Index (DI). As shown in Figure 6, the LAM for MSAAN-light covers a broader and more relevant region of the input image compared to RFDN, SAFMN, and PAN. The higher DI value for MSAAN-light indicates that our MSAA module enables the network to utilize contextual information from a wider pixel range for reconstruction, thanks to its effective integration of multi-scale and non-local features.

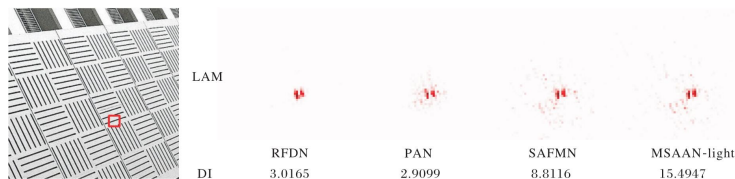


Figure 6: Local Attribution Maps (LAM) of MSAAN-light and contrastive methods

## 4.4 Conclusion of Experiments

Extensive experiments validate the effectiveness of the proposed MSAAN. Ablation studies confirm the contribution of each component (LEB, MSAA, FIGFF). Quantitative comparisons show that both MSAAN-light and MSAAN achieve state-of-the-art performance with high efficiency. Qualitative visual comparisons and LAM analysis further demonstrate the superior perceptual quality and more comprehensive use of image context by our method.

## 5 Conclusion

In this paper, we address the critical trade-off between reconstruction quality and model complexity in image super-resolution by proposing a novel Multi-scale Spatial Adaptive Attention Network (MSAAN). The core of our method is a carefully designed Multi-scale Spatial Adaptive Attention Module (MSAA), which effectively unifies the modeling of local high-frequency details and long-range contextual dependencies. The MSAA integrates a Global Feature Modulation Module (GFM) to learn coherent texture structures and a Multi-scale Feature Aggregation Module (MFA) to adaptively fuse features across scales. Furthermore, the auxiliary Local Enhancement Block (LEB) and Feature Interactive Gated Feed-Forward Module (FIGFF) are introduced to strengthen

local geometric perception and enhance feature transformation efficiency, respectively.

Extensive experiments on multiple benchmark datasets demonstrate the superiority of the proposed MSAAN. Both the lightweight (MSAAN-light) and standard (MSAAN) versions achieve state-of-the-art or highly competitive performance in terms of PSNR and SSIM metrics while maintaining significantly lower parameter counts and computational costs compared to contemporary methods. Ablation studies validate the effectiveness of each proposed component. Visual comparisons and Local Attribution Map analysis further confirm that our network reconstructs images with sharper edges and more authentic textures by leveraging more comprehensive contextual information.

While the current model performs well on standard benchmarks, future work will focus on enhancing its generalization capability. This includes training with more diverse and realistic degradation models to better handle complex real-world scenarios. Exploring the integration of advanced attention mechanisms or dynamic network structures could also be promising directions for further improving performance and efficiency.

## References

- [1] J. Redmon, S. Divvala, R. Girshick, and A. Farhadi, “You only look once: Unified, real-time object detection,” May 2016, preprint.
- [2] H. Yu, Y. Wu, F. Shi, L. Liao, J. Lu, X. Ge, H. Wang, M. Zhuo, X. Wu, X. Fei *et al.*, “Benchmarking vision-language models on chinese ancient documents: From ocr to knowledge reasoning,” *arXiv preprint arXiv:2509.09731*, 2025.
- [3] H. Feng, Z. Wang, J. Tang, J. Lu, W. Zhou, H. Li, and C. Huang, “Unidoc: A universal large multimodal model for simultaneous text detection, recognition, spotting and understanding,” *arXiv preprint arXiv:2308.11592*, 2023.
- [4] R. Teknium, J. Quesnelle, and C. Guang, “Hermes 3 technical report,” 2024. [Online]. Available: <https://arxiv.org/abs/2408.11857>
- [5] T. Li, G. Zhang, Q. D. Do, X. Yue, and W. Chen, “Long-context llms struggle with long in-context learning,” 2024. [Online]. Available: <https://arxiv.org/abs/2404.02060>
- [6] J. Achiam, S. Adler, S. Agarwal, L. Ahmad, I. Akkaya, F. L. Aleman, D. Almeida, J. Altschmidt, S. Altman, S. Anadkat *et al.*, “Gpt-4 technical report,” *arXiv preprint arXiv:2303.08774*, 2023.
- [7] S. Huang, Y. Wang, H. Luo, H. Jing, C. Qin, and J. Tang, “Mindev: Multi-modal integrated diffusion framework for video reconstruction from eeg signals,” pp. 3350–3359, 2025.
- [8] Y. Liu, J. Zhang, D. Peng, M. Huang, X. Wang, J. Tang, C. Huang, D. Lin, C. Shen, X. Bai *et al.*, “Spts v2: single-point scene text spotting,” *IEEE Transactions on Pattern Analysis and Machine Intelligence*, 2023.
- [9] W. Sun, X.-M. Dong, B. Cui, and J. Tang, “Attentive eraser: Unleashing diffusion model’s object removal potential via self-attention redirection guidance,” vol. 39, no. 19, pp. 20 734–20 742, 2025.
- [10] Z. Xiao, Z. Mai, Z. Xu, Y. Cui, and J. Li, “Corporate event predictions using large language models,” in *2023 10th International Conference on Soft Computing & Machine Intelligence (ISCMI)*, 2023, pp. 193–197.
- [11] Y. Chen, V. Shah, and A. Ritter, “Translation and fusion improves zero-shot cross-lingual information extraction,” 2024. [Online]. Available: <https://arxiv.org/abs/2305.13582>
- [12] Z. Guo, L. Xia, Y. Yu, T. Ao, and C. Huang, “Lightrag: Simple and fast retrieval-augmented generation,” 2024. [Online]. Available: <https://arxiv.org/abs/2410.05779>

- [13] J. Lu, H. Yu, Y. Wang, Y. Ye, J. Tang, Z. Yang, B. Wu, Q. Liu, H. Feng, H. Wang *et al.*, “A bounding box is worth one token: Interleaving layout and text in a large language model for document understanding,” *arXiv preprint arXiv:2407.01976*, 2024.
- [14] Y. Gao, Y. Xiong, X. Gao, K. Jia, J. Pan, Y. Bi, Y. Dai, J. Sun, and H. Wang, “Retrieval-augmented generation for large language models: A survey,” *arXiv preprint arXiv:2312.10997*, 2023.
- [15] B. Shan, X. Fei, W. Shi, A.-L. Wang, G. Tang, L. Liao, J. Tang, X. Bai, and C. Huang, “Mctbench: Multimodal cognition towards text-rich visual scenes benchmark,” *arXiv preprint arXiv:2410.11538*, 2024.
- [16] D. Guo, F. Wu, F. Zhu, F. Leng, G. Shi, H. Chen, H. Fan, J. Wang, J. Jiang, J. Wang *et al.*, “Seed1. 5-vl technical report,” *arXiv preprint arXiv:2505.07062*, 2025.
- [17] J. Lu, H. Yu, S. Xu, S. Ran, G. Tang, S. Wang, B. Shan, T. Fu, H. Feng, J. Tang *et al.*, “Prolonged reasoning is not all you need: Certainty-based adaptive routing for efficient llm/mlm reasoning,” *arXiv preprint arXiv:2505.15154*, 2025.
- [18] L. Wang, N. Yang, X. Huang, L. Yang, R. Majumder, and F. Wei, “Improving text embeddings with large language models,” *arXiv preprint arXiv:2401.00368*, 2023.
- [19] A.-L. Wang, B. Shan, W. Shi, K.-Y. Lin, X. Fei, G. Tang, L. Liao, J. Tang, C. Huang, and W.-S. Zheng, “Pargo: Bridging vision-language with partial and global views,” vol. 39, no. 7, pp. 7491–7499, 2025.
- [20] J. Tang, W. Zhang, H. Liu, M. Yang, B. Jiang, G. Hu, and X. Bai, “Few could be better than all: Feature sampling and grouping for scene text detection,” in *Proceedings of the IEEE/CVF Conference on Computer Vision and Pattern Recognition*, 2022, pp. 4563–4572.
- [21] J. Tang, W. Qian, L. Song, X. Dong, L. Li, and X. Bai, “Optimal boxes: boosting end-to-end scene text recognition by adjusting annotated bounding boxes via reinforcement learning,” in *European Conference on Computer Vision*. Springer, 2022, pp. 233–248.
- [22] J. Ho, A. Jain, and P. Abbeel, “Denoising diffusion probabilistic models,” *Advances in neural information processing systems*, vol. 33, pp. 6840–6851, 2020.
- [23] J. Tang, W. Du, B. Wang, W. Zhou, S. Mei, T. Xue, X. Xu, and H. Zhang, “Character recognition competition for street view shop signs,” *National Science Review*, vol. 10, no. 6, p. nwad141, 2023.

- [24] A.-L. Wang, J. Tang, L. Lei, H. Feng, Q. Liu, X. Fei, J. Lu, H. Wang, W. Liu, H. Liu *et al.*, “Wilddoc: How far are we from achieving comprehensive and robust document understanding in the wild?” *arXiv preprint arXiv:2505.11015*, 2025.
- [25] X. Fei, J. Lu, Q. Sun, H. Feng, Y. Wang, W. Shi, A.-L. Wang, J. Tang, and C. Huang, “Advancing sequential numerical prediction in autoregressive models,” *arXiv preprint arXiv:2505.13077*, 2025.
- [26] H. Feng, Q. Liu, H. Liu, J. Tang, W. Zhou, H. Li, and C. Huang, “Docpedia: Unleashing the power of large multimodal model in the frequency domain for versatile document understanding,” *Science China Information Sciences*, vol. 67, no. 12, pp. 1–14, 2024.
- [27] L. Fu, B. Yang, Z. Kuang, J. Song, Y. Li, L. Zhu, Q. Luo, X. Wang, H. Lu, M. Huang *et al.*, “Ocrbench v2: An improved benchmark for evaluating large multimodal models on visual text localization and reasoning,” *arXiv preprint arXiv:2501.00321*, 2024.
- [28] J. Fang, Z. Xiao, Y. Wu, J. Zhang, Z. Xu, and Z. Mai, “A comparative study of sequential deep learning models in financial time series forecasting,” in *2024 11th International Conference on Soft Computing & Machine Intelligence (ISCM)*, 2024, pp. 22–26.
- [29] J. Wu, J. Zhu, Y. Qi, J. Chen, M. Xu, F. Menolascina, and V. Grau, “Medical graph rag: Towards safe medical large language model via graph retrieval-augmented generation,” 2024. [Online]. Available: <https://arxiv.org/abs/2408.04187>
- [30] Z. Zhao, J. Tang, B. Wu, C. Lin, S. Wei, H. Liu, X. Tan, Z. Zhang, C. Huang, and Y. Xie, “Harmonizing visual text comprehension and generation,” *arXiv preprint arXiv:2407.16364*, 2024.
- [31] W. Zhao, H. Feng, Q. Liu, J. Tang, B. Wu, L. Liao, S. Wei, Y. Ye, H. Liu, W. Zhou *et al.*, “Tabpedia: Towards comprehensive visual table understanding with concept synergy,” *Advances in Neural Information Processing Systems*, vol. 37, pp. 7185–7212, 2025.
- [32] Z. Zhao, J. Tang, C. Lin, B. Wu, C. Huang, H. Liu, X. Tan, Z. Zhang, and Y. Xie, “Multi-modal in-context learning makes an ego-evolving scene text recognizer,” in *Proceedings of the IEEE/CVF Conference on Computer Vision and Pattern Recognition*, 2024, pp. 15 567–15 576.
- [33] C. Wang, C. Nie, and Y. Liu, “Evaluating supervised learning models for fraud detection: A comparative study of classical and deep architectures on imbalanced transaction data,” *arXiv preprint arXiv:2505.22521*, 2025.
- [34] J. Tang, C. Lin, Z. Zhao, S. Wei, B. Wu, Q. Liu, H. Feng, Y. Li, S. Wang, L. Liao *et al.*, “Textsquare: Scaling up text-centric visual instruction tuning,” *arXiv preprint arXiv:2404.12803*, 2024.

- [35] J. Tang, S. Qiao, B. Cui, Y. Ma, S. Zhang, and D. Kanoulas, “You can even annotate text with voice: Transcription-only-supervised text spotting,” in *Proceedings of the 30th ACM International Conference on Multimedia*, ser. MM ’22. New York, NY, USA: Association for Computing Machinery, 2022, pp. 4154–4163. [Online]. Available: <https://doi.org/10.1145/3503161.3547787>
- [36] M. T. Khan, L. Chen, Y. H. Ng, W. Feng, N. Y. J. Tan, and S. K. Moon, “Fine-tuning vision-language model for automated engineering drawing information extraction,” 2024, preprint.
- [37] W. Jia, J. Lu, H. Yu, S. Wang, G. Tang, A.-L. Wang, W. Yin, D. Yang, Y. Nie, B. Shan *et al.*, “Meml-grpo: Heterogeneous multi-expert mutual learning for rlvr advancement,” *arXiv preprint arXiv:2508.09670*, 2025.
- [38] A. S. Steyn, “Afrikaans, inc.: the afrikaans culture industry after apartheid,” *Social Dynamics*, vol. 42, pp. 481–503, 2016. [Online]. Available: <https://api.semanticscholar.org/CorpusID:152269054>
- [39] H. Feng, S. Wei, X. Fei, W. Shi, Y. Han, L. Liao, J. Lu, B. Wu, Q. Liu, C. Lin *et al.*, “Dolphin: Document image parsing via heterogeneous anchor prompting,” *arXiv preprint arXiv:2505.14059*, 2025.
- [40] H. Wang, Y. Ye, B. Li, Y. Nie, J. Lu, J. Tang, Y. Wang, and C. Huang, “Vision as lora,” *arXiv preprint arXiv:2503.20680*, 2025.
- [41] S. Veturi, S. Vaichal, R. L. Jagadheesh, N. I. Tripto, and N. Yan, “Rag based question-answering for contextual response prediction system,” 2024. [Online]. Available: <https://arxiv.org/abs/2409.03708>
- [42] R. Rombach, A. Blattmann, D. Lorenz, P. Esser, and B. Ommer, “High-resolution image synthesis with latent diffusion models,” *Proceedings of the IEEE/CVF conference on computer vision and pattern recognition*, pp. 10 684–10 695, 2022.
- [43] X. Li, T. Mangin, S. Saha, R. Mohammed, E. Blanchard, D. Tang, H. Poppe, O. Choi, K. Kelly, and R. Whitaker, “Real-time idling vehicles detection using combined audio-visual deep learning,” in *Emerging Cutting-Edge Developments in Intelligent Traffic and Transportation Systems*. IOS Press, 2024, pp. 142–158.
- [44] H. Jiang, Q. Wu, X. Luo, D. Li, C.-Y. Lin, Y. Yang, and L. Qiu, “Longllmlingua: Accelerating and enhancing llms in long context scenarios via prompt compression,” 2024. [Online]. Available: <https://arxiv.org/abs/2310.06839>
- [45] “torchvision.transforms torchvision master documentation,” <https://pytorch.org/vision/0.9/transforms.html>, accessed: 2025-03-22.

- [46] P. Authors, “Paddleocr: A versatile ocr toolkit with 80+ languages recognition,” 2023.
- [47] D. Jinensibieke, M. Maimaiti, W. Xiao, Y. Zheng, and X. Wang, “How good are llms at relation extraction under low-resource scenario? comprehensive evaluation,” 2024. [Online]. Available: <https://arxiv.org/abs/2406.11162>
- [48] Z. Mai, J. Zhang, Z. Xu, and Z. Xiao, “Financial sentiment analysis meets llama 3: A comprehensive analysis,” in *Proceedings of the 2024 7th International Conference on Machine Learning and Machine Intelligence (MLMI)*, ser. MLMI ’24. New York, NY, USA: Association for Computing Machinery, 2024, p. 171–175. [Online]. Available: <https://doi.org/10.1145/3696271.3696299>
- [49] L. Zheng, W.-L. Chiang, Y. Sheng, S. Zhuang, Z. Wu, Y. Zhuang, Z. Lin, Z. Li, D. Li, E. Xing *et al.*, “Judging llm-as-a-judge with mt-bench and chatbot arena,” *Advances in Neural Information Processing Systems*, vol. 36, pp. 46 595–46 623, 2023.
- [50] A. Dubey, A. Jauhri, A. Pandey, A. Kadian, A. Al-Dahle, A. Letman, A. Mathur, A. Schelten, A. Yang, A. Fan *et al.*, “The llama 3 herd of models,” *arXiv preprint arXiv:2407.21783*, 2024.
- [51] Z. Xiao, Z. Mai, Y. Cui, Z. Xu, and J. Li, “Short interest trend prediction with large language models,” in *Proceedings of the 2024 International Conference on Innovation in Artificial Intelligence*, ser. ICAI ’24. New York, NY, USA: Association for Computing Machinery, 2024, p. 1. [Online]. Available: <https://doi.org/10.1145/3655497.3655500>
- [52] W. Sun and Y. Gao, “A datum-based model for practicing geometric dimensioning and tolerancing,” *Journal of Engineering Technology*, vol. 35, pp. 38–47, Sep 2018.
- [53] W. Zhang, G. Zhai, Y. Wei, X. Yang, and K. Ma, “Blind image quality assessment via vision-language correspondence: A multitask learning perspective,” pp. 14 071–14 081, 2023.
- [54] Z. Xiao, Z. Mai, Z. Xu, Y. Kwon, and J. Li, “Short interest trend prediction,” in *2024 6th International Conference on Natural Language Processing (ICNLP)*, 2024, pp. 352–356.
- [55] Y. Wu, Z. Xiao, J. Zhang, Z. Mai, and Z. Xu, “Can llama 3 understand monetary policy?” in *2024 17th International Conference on Advanced Computer Theory and Engineering (ICACTE)*, 2024, pp. 145–149.
- [56] Z. Mai, J. Zhang, Z. Xu, and Z. Xiao, “Is llama 3 good at sarcasm detection? a comprehensive study,” in *Proceedings of the 2024 7th International Conference on Machine Learning and Machine Intelligence (MLMI)*, ser. MLMI ’24. New York, NY, USA: Association

- for Computing Machinery, 2024, p. 141–145. [Online]. Available: <https://doi.org/10.1145/3696271.3696294>
- [57] Y. Wu, X. Xie, Z. Xiao, J. Zhang, Z. Xu, and Z. Mai, “Recent technologies in differential privacy for nlp applications,” in *2024 11th International Conference on Soft Computing & Machine Intelligence (ISCMI)*, 2024, pp. 242–246.
- [58] J. Xing, Z. Xiao, Y. Wu, J. Zhang, Z. Xu, and Z. Mai, “Network traffic forecasting via fuzzy spatial-temporal fusion graph neural networks,” in *2024 11th International Conference on Soft Computing & Machine Intelligence (ISCMI)*, 2024, pp. 282–286.
- [59] J. Tang, Q. Liu, Y. Ye, J. Lu, S. Wei, C. Lin, W. Li, M. F. F. B. Mahmood, H. Feng, Z. Zhao *et al.*, “Mtvqa: Benchmarking multilingual text-centric visual question answering,” *arXiv preprint arXiv:2405.11985*, 2024.
- [60] C. Yu, Z. Xiao, J. Zhang, Z. Xu, and Z. Mai, “Comparative study of intersection management algorithms for autonomous vehicles,” in *2024 6th International Conference on Machine Learning, Big Data and Business Intelligence (MLBDBI)*, 2024, pp. 290–294.
- [61] K. Liu, Z. Chen, M. Li, J. Tang, D. Yang, and L. Zhang, “Resolving evidence sparsity: Agentic context engineering for long-document understanding,” *arXiv preprint arXiv:2511.22850*, 2025.
- [62] “AutoCAD mechanical 2022 help — about balloons (autocad mechanical toolset) — autodesk,” [https://help.autodesk.com/view/AMECH\\_PP/2022/ENU/?guid=GUID-F12F0EAO-0810-42EE-A3FE-327041AFAEEE](https://help.autodesk.com/view/AMECH_PP/2022/ENU/?guid=GUID-F12F0EAO-0810-42EE-A3FE-327041AFAEEE), 2022, accessed: 2024-09-27.
- [63] F. Alam, S. A. Chowdhury, S. Boughorbel, and M. Hasanain, “Llms for low resource languages in multilingual, multimodal and dialectal settings,” in *Conference of the European Chapter of the Association for Computational Linguistics*, 2024. [Online]. Available: <https://api.semanticscholar.org/CorpusID:268417133>
- [64] Anthropic, “Introducing contextual retrieval,” <https://www.anthropic.com/news/contextual-retrieval>, 2024, accessed: 2024-11-02.
- [65] “Leading image & video data annotation platform CVAT,” <https://www.cvat.ai>, 2024, accessed: 2025-03-22.
- [66] J. Gao, D. T. Zheng, N. Gindy, and D. Clark, “Extraction/conversion of geometric dimensions and tolerances for machining features,” *International Journal of Advanced Manufacturing Technology*, vol. 26, no. 4, pp. 405–414, Aug 2005.

- [67] D. Edge, H. Trinh, N. Cheng, J. Bradley, A. Chao, A. Mody, S. Truitt, and J. Larson, “From local to global: A graph rag approach to query-focused summarization,” *arXiv preprint arXiv:2404.16130*, 2024.
- [68] M. Günther, I. Mohr, D. J. Williams, B. Wang, and H. Xiao, “Late chunking: contextual chunk embeddings using long-context embedding models,” *arXiv preprint arXiv:2409.04701*, 2024.
- [69] G. Jhajj and Y. Nomura, “Jack and the beanstalk: Towards question answering in plant biology.” [Online]. Available: <https://api.semanticscholar.org/CorpusID:274567831>
- [70] P. Lewis, E. Perez, A. Piktus, F. Petroni, V. Karpukhin, N. Goyal, H. Küttler, M. Lewis, W.-t. Yih, T. Rocktäschel *et al.*, “Retrieval-augmented generation for knowledge-intensive nlp tasks,” *Advances in Neural Information Processing Systems*, vol. 33, pp. 9459–9474, 2020.
- [71] X. Li, R. Whitaker, and T. Tasdizen, “Audio and multiscale visual cues driven cross-modal transformer for idling vehicle detection,” *arXiv preprint arXiv:2504.16102*, 2025.
- [72] X. Li, R. Mohammed, T. Mangin, S. Saha, K. Kelly, R. Whitaker, and T. Tasdizen, “Joint audio-visual idling vehicle detection with streamlined input dependencies,” in *Proceedings of the Winter Conference on Applications of Computer Vision*, 2025, pp. 885–894.
- [73] Y.-H. Lin, Y.-H. Ting, Y.-C. Huang, K.-L. Cheng, and W.-R. Jong, “Integration of deep learning for automatic recognition of 2D engineering drawings,” *Machines*, vol. 11, no. 8, Aug 2023.
- [74] S. Liu, Y. Zhang, X. Li, Y. Liu, C. Feng, and H. Yang, “Gated multimodal graph learning for personalized recommendation,” *INNO-PRESS: Journal of Emerging Applied AI*, vol. 1, no. 1, 2025.
- [75] Y. Liu, X. Qin, Y. Gao, X. Li, and C. Feng, “Setransformer: A hybrid attention-based architecture for robust human activity recognition,” *INNO-PRESS: Journal of Emerging Applied AI*, vol. 1, no. 1, 2025.
- [76] “Data management and SPC software,” <https://measurlink.com/>, accessed: 2024-09-27.
- [77] K. Niu, H. Yu, Z. Chen, Z. Yao, W. Jia, X. Ge, J. Tang, B. Cui, B. Li, and X. Xue, “Cme-cad: Heterogeneous collaborative multi-expert reinforcement learning for cad code generation,” *arXiv preprint arXiv:2512.23333*, 2025.
- [78] J. Austen, *Pride and Prejudice*. Urbana, Illinois: Project Gutenberg, 2006. [Online]. Available: <https://www.gutenberg.org/ebooks/1342>

- [79] tesseract-ocr, “tesseract-ocr/tesseract,” <https://github.com/tesseract-ocr/tesseract>, 2024, accessed: 2024-09-27.
- [80] M. Trajanoska, R. Stojanov, and D. Trajanov, “Enhancing knowledge graph construction using large language models,” 2023. [Online]. Available: <https://arxiv.org/abs/2305.04676>
- [81] Y. Wang, J. Zhong, and R. Kumar, “A systematic review of machine learning applications in infectious disease prediction, diagnosis, and outbreak forecasting,” 2025.
- [82] J. Wang, Y. Liang, F. Meng, Z. Sun, H. Shi, Z. Li, J. Xu, J. Qu, and J. Zhou, “Is chatgpt a good nlg evaluator? a preliminary study,” *arXiv preprint arXiv:2303.04048*, 2023.
- [83] J. Wang, Z. Zhang, Y. He, Y. Song, T. Shi, Y. Li, H. Xu, K. Wu, G. Qian, Q. Chen *et al.*, “Enhancing code llms with reinforcement learning in code generation,” *arXiv preprint arXiv:2412.20367*, 2024.
- [84] Y. Wang, T. Zhao, and X. Wang, “Fine-grained heartbeat waveform monitoring with rfid: A latent diffusion model,” pp. 86–91, 2025.
- [85] K. Wataoka, T. Takahashi, and R. Ri, “Self-preference bias in llm-as-a-judge,” *arXiv preprint arXiv:2410.21819*, 2024.
- [86] Y. Xu *et al.*, “Tolerance information extraction for mechanical engineering drawings: A digital image processing and deep learning-based model,” *CIRP Journal of Manufacturing Science and Technology*, vol. 50, pp. 55–64, Jun 2024.
- [87] J. Zhong and Y. Wang, “Enhancing thyroid disease prediction using machine learning: A comparative study of ensemble models and class balancing techniques,” 2025.
- [88] R.-C. Chang and J. Zhang, “Communitykg-rag: Leveraging community structures in knowledge graphs for advanced retrieval-augmented generation in fact-checking,” 2024. [Online]. Available: <https://arxiv.org/abs/2408.08535>
- [89] S. Es, J. James, L. Espinosa-Anke, and S. Schockaert, “Ragas: Automated evaluation of retrieval augmented generation,” 2023. [Online]. Available: <https://arxiv.org/abs/2309.15217>
- [90] Z. Xiao, Y. Cui, Z. Mai, Z. Xu, and J. Li, “Corporate event prediction using earning call transcripts,” in *Information Management and Big Data*, J. A. Lossio-Ventura, E. Ceh-Varela, G. Vargas-Solar, R. Marcacini, C. Tandonki, H. Calvo, and H. Alatrística-Salas, Eds. Cham: Springer Nature Switzerland, 2024, pp. 261–272.

- [91] Z. Xiao, Y. Huang, and E. Blanco, “Analyzing large language models’ capability in location prediction,” in *Proceedings of the 2024 Joint International Conference on Computational Linguistics, Language Resources and Evaluation (LREC-COLING 2024)*, N. Calzolari, M.-Y. Kan, V. Hoste, A. Lenci, S. Sakti, and N. Xue, Eds. Torino, Italia: ELRA and ICCL, May 2024, pp. 951–958. [Online]. Available: <https://aclanthology.org/2024.lrec-main.85>
- [92] —, “Context helps determine spatial knowledge from tweets,” in *Findings of the Association for Computational Linguistics: IJCNLP-AACL 2023 (Findings)*, J. C. Park, Y. Arase, B. Hu, W. Lu, D. Wijaya, A. Purwarianti, and A. A. Krisnadhi, Eds. Nusa Dua, Bali: Association for Computational Linguistics, Nov. 2023, pp. 149–160. [Online]. Available: <https://aclanthology.org/2023.findings-ijcnlp.13>
- [93] Z. Xiao and E. Blanco, “Are people located in the places they mention in their tweets? a multimodal approach,” in *Proceedings of the 29th International Conference on Computational Linguistics*, N. Calzolari, C.-R. Huang, H. Kim, J. Pustejovsky, L. Wanner, K.-S. Choi, P.-M. Ryu, H.-H. Chen, L. Donatelli, H. Ji, S. Kurohashi, P. Paggio, N. Xue, S. Kim, Y. Hahm, Z. He, T. K. Lee, E. Santus, F. Bond, and S.-H. Na, Eds. Gyeongju, Republic of Korea: International Committee on Computational Linguistics, Oct. 2022, pp. 2561–2571. [Online]. Available: <https://aclanthology.org/2022.coling-1.226>
- [94] J. Zhang, Z. Mai, Z. Xu, and Z. Xiao, “Is llama 3 good at identifying emotion? a comprehensive study,” in *Proceedings of the 2024 7th International Conference on Machine Learning and Machine Intelligence (MLMI)*, ser. MLMI ’24. New York, NY, USA: Association for Computing Machinery, 2024, p. 128–132. [Online]. Available: <https://doi.org/10.1145/3696271.3696292>
- [95] Y. Wu, X. Xie, C. Yu, Z. Xiao, J. Zhang, Z. Xu, and Z. Mai, “A survey on origin-destination flow prediction,” in *2024 11th International Conference on Soft Computing & Machine Intelligence (ISCFMI)*, 2024, pp. 48–52.
- [96] C. Yu, X. Xie, Z. Xiao, Y. Wu, J. Zhang, Z. Xu, and Z. Mai, “Crime prediction using spatial-temporal synchronous graph convolutional networks,” in *2024 11th International Conference on Soft Computing & Machine Intelligence (ISCFMI)*, 2024, pp. 129–133.
- [97] C. Yu, Z. Xiao, Y. Wu, J. Zhang, Z. Xu, and Z. Mai, “A social value orientation-based priority swapping algorithm for efficient autonomous intersection management,” in *2024 11th International Conference on Soft Computing & Machine Intelligence (ISCFMI)*, 2024, pp. 158–162.
- [98] J. Zhang, B. Wang, D. Wang, S. Fu, K. Lu, Y. Wan, and J. Xie, “An sdr-based lte system for unmanned aerial systems,” in *2022 International Conference on Unmanned Aircraft Systems (ICUAS)*, 2022, pp. 1448–1454.

- [99] D. Wang, B. Wang, J. Zhang, K. Lu, J. Xie, Y. Wan, and S. Fu, “Cfl-hc: A coded federated learning framework for heterogeneous computing scenarios,” in *2021 IEEE Global Communications Conference (GLOBECOM)*, 2021, pp. 1–6.